

*Electronic Supplementary Information for:*

**Multi-Component Crystals Containing Urea:  
Mechanochemical Synthesis and Characterization  
by  $^{35}\text{Cl}$  Solid-State NMR Spectroscopy and DFT Calculations**

Cameron S. Vojvodin,<sup>1,2</sup> Sean T. Holmes,<sup>1,2</sup> Lara K. Watanabe,<sup>3</sup>

Jeremy M. Rawson,<sup>3</sup> Robert W. Schurko<sup>1,2\*</sup>

<sup>1</sup> Department of Chemistry & Biochemistry, Florida State University, Tallahassee, FL 32306

<sup>2</sup> National High Magnetic Field Laboratory, Tallahassee, FL 32310

<sup>3</sup> Department of Chemistry & Biochemistry, University of Windsor, Windsor, ON, N9B 3P4

\*Author to whom correspondence should be addressed.

E-mail: [rschurko@fsu.edu](mailto:rschurko@fsu.edu)

## Supplementary Information

### Table of Contents

<b>Figure S1.</b> Experimental PXRD patterns for (A, purple) $\text{NH}_4\text{Cl}$ , (B, green) urea, (C, red) $\text{NPr}_4\text{Cl}$ , and (D, blue) $\text{NEt}_4\text{Cl}\cdot\text{H}_2\text{O}$ , as well as simulated PXRD patterns based on previously reported or novel crystal structures (black). <sup>109,111</sup> .....	4
<b>Table S1.</b> Experimental conditions used in ball milling experiments <sup>a</sup> for the syntheses of all MCCs described in this work. All reactions were scaled to <i>ca.</i> 200 mg of total solids. ....	5
<b>Supplement S1. Euler Angle Conventions.</b> .....	6
<b>Figure S2.</b> Experimental $^1\text{H}\rightarrow^{13}\text{C}\{^1\text{H}\}$ CP/MAS spectra for (A) $\text{NEt}_4\text{Cl}\cdot\text{H}_2\text{O}$ and (B) $\text{NPr}_4\text{Cl}$ acquired at 14.1 T ( $\nu_{\text{rot}} = 6$ kHz). Spinning sidebands are denoted by asterisks (*)......	7
<b>Figure S3.</b> Experimental $^1\text{H}\rightarrow^{13}\text{C}\{^1\text{H}\}$ CP/MAS spectra of (A) $\text{NH}_4\text{Cl}:\text{Urea}$ , (B) $\text{NEt}_4\text{Cl}:2\text{Urea}$ , (C) $\text{NEt}_4\text{Cl}:\text{Urea}\cdot 2\text{H}_2\text{O}$ , (D) $\text{NPr}_4\text{Cl}:2\text{Urea}$ , and (E) $\text{NPr}_4\text{Cl}:3\text{Urea}$ acquired at 14.1 T ( $\nu_{\text{rot}} = 6$ kHz). Spinning sidebands are denoted by asterisks (*). ....	8
<b>Table S2.</b> Summary of experimental $^{13}\text{C}$ chemical shifts. ....	9
<b>Figure S4.</b> Images of the unit cells of (A) $\text{NH}_4\text{Cl}:\text{Urea}$ and (B) $\text{NPr}_4\text{Cl}$ . ....	10
<b>Table S3.</b> Crystal structure details for $\text{NH}_4\text{Cl}:\text{Urea}$ and $\text{NPr}_4\text{Cl}$ . ....	11
<b>Table S4.</b> Experimental $^{35}\text{Cl}$ EFG and CS tensor parameters for $\text{NEt}_4\text{Cl}\cdot\text{H}_2\text{O}$ . <sup>a</sup> .....	12
<b>Figure S5.</b> Experimental PXRD patterns for (A, purple) $\text{NPr}_4\text{Cl}:3\text{Urea}$ , (B, green) $\text{NEt}_4\text{Cl}:\text{Urea}\cdot 2\text{H}_2\text{O}$ , (C, red) $\text{NPr}_4\text{Cl}:2\text{Urea}$ , and (D, blue) $\text{NEt}_4\text{Cl}:2\text{Urea}$ , as well as simulated PXRD patterns based on previously-reported crystal structures (black). <sup>112–114</sup> .....	13
<b>Table S5.</b> Summary of crystallographic details for all $\text{NR}_4\text{Cl}:x\text{Urea}\cdot y\text{H}_2\text{O}$ MCCs and precursors discussed in this work. ....	14
<b>Figure S6.</b> Experimental PXRD patterns for $\text{NH}_4\text{Cl}:\text{Urea}$ at 1, 5, 10, 20, 30, and 40 minutes with a constant milling frequency of 30 Hz. Optimal milling time is marked with an asterisk (*). Simulated reference PXRD patterns for urea, $\text{NH}_4\text{Cl}$ , and $\text{NH}_4\text{Cl}:\text{Urea}$ are also shown. ....	15
<b>Figure S7.</b> Experimental PXRD patterns for $\text{NEt}_4\text{Cl}:2\text{Urea}$ at 1, 5, 10, 20, 30, and 40 minutes with a constant milling frequency of 30 Hz. Optimal milling time is marked with an asterisk (*). Simulated reference PXRD patterns for urea, $\text{NEt}_4\text{Cl}\cdot\text{H}_2\text{O}$ , and $\text{NEt}_4\text{Cl}:2\text{Urea}$ are also shown. .	16
<b>Figure S8.</b> Experimental PXRD patterns for $\text{NEt}_4\text{Cl}:\text{Urea}\cdot 2\text{H}_2\text{O}$ at 1, 5, 10, 20, 30, and 40 minutes with a constant milling frequency of 30 Hz. Optimal milling time is marked with an asterisk (*). Simulated reference PXRD patterns for urea, $\text{NEt}_4\text{Cl}\cdot\text{H}_2\text{O}$ , and $\text{NEt}_4\text{Cl}:\text{Urea}\cdot 2\text{H}_2\text{O}$ are also shown.....	17
<b>Figure S9.</b> Experimental PXRD patterns for $\text{NPr}_4\text{Cl}:2\text{Urea}$ at 1, 5, 10, 20, 30, and 40 minutes with a constant milling frequency of 30 Hz. Optimal milling time is marked with an asterisk (*). Simulated reference PXRD patterns for urea, $\text{NPr}_4\text{Cl}$ , and $\text{NPr}_4\text{Cl}:2\text{Urea}$ are also shown. ....	18

<b>Figure S10.</b> Experimental PXRD patterns for $\text{NPr}_4\text{Cl}:3\text{Urea}$ at 1, 5, 10, 20, 30, and 40 minutes with a constant milling frequency of 30 Hz. Optimal milling time is marked with an asterisk (*). Simulated reference PXRD patterns for urea, $\text{NPr}_4\text{Cl}$ , and $\text{NPr}_4\text{Cl}:3\text{Urea}$ are also shown. ....	19
<b>Figure S11.</b> PXRD patterns of the mechanochemically synthesized product of 1 molar eq. urea, 1 molar eq. $\text{NEt}_4\text{Cl}\cdot\text{H}_2\text{O}$ , and 0 (A), 1 (B), and 2 (C) molar eq. $\text{H}_2\text{O}$ . ....	20
<b>Supplement S2. Definition of the RMS EFG Distance.</b> .....	21
<b>Figure S12.</b> Correlations between calculated and experimental principal values of $^{35}\text{Cl}$ chemical shift tensors for tetraethyl and tetrapropyl $\text{NR}_4\text{Cl}:x\text{Urea}\cdot y\text{H}_2\text{O}$ MCCs. Calculations are shown for XRD-derived structures (blue) and DFT-D2* structures (red).....	22
<b>Supplement S3. Definition of the RMS CS Distance.</b> .....	23
<b>Figure S13.</b> Experimental and simulated PXRD patterns of products from MS and crystallization from solution, as well as simulated PXRD patterns for $\text{NH}_4\text{Cl}:\text{Urea}$ . Both slow evaporation (purple) and ball milling (brown) products from preparations of $\text{NH}_4\text{Cl}:\text{Urea}$ are compared to simulations of the three reported crystal structures, black (URAMCL), red (URAMCL01), and green (URAMCL02), <sup>123–125</sup> and our <i>Pmna</i> crystal structure (blue).....	24
<b>Table S6.</b> Calculated $^{35}\text{Cl}$ EFG tensor parameters for all available structures of $\text{NH}_4\text{Cl}:\text{Urea}$ , as refined at the DFT-D2* level.....	25
<b>Figure S14.</b> $^{35}\text{Cl}$ EFG tensor orientations for $\text{NH}_4\text{Cl}:\text{Urea}$ obtained from model structures from our crystal structure that were geometry optimized at the DFT-D2* level. The $\text{H}\cdots\text{Cl}^-$ hydrogen bonds ( $< 2.6 \text{ \AA}$ ) are shown in black. The orientations of the three principal components of the EFG tensor ( $V_{11}$ , $V_{22}$ , and $V_{33}$ ) are shown in yellow. ....	26
<b>Table S7.</b> Acquisition parameters for all $^{35}\text{Cl}\{^1\text{H}\}$ Hahn-echo SSNMR spectra.....	27
<b>Table S8.</b> Acquisition parameters for all $^1\text{H}\rightarrow^{13}\text{C}\{^1\text{H}\}$ CP/MAS SSNMR spectra. ....	28

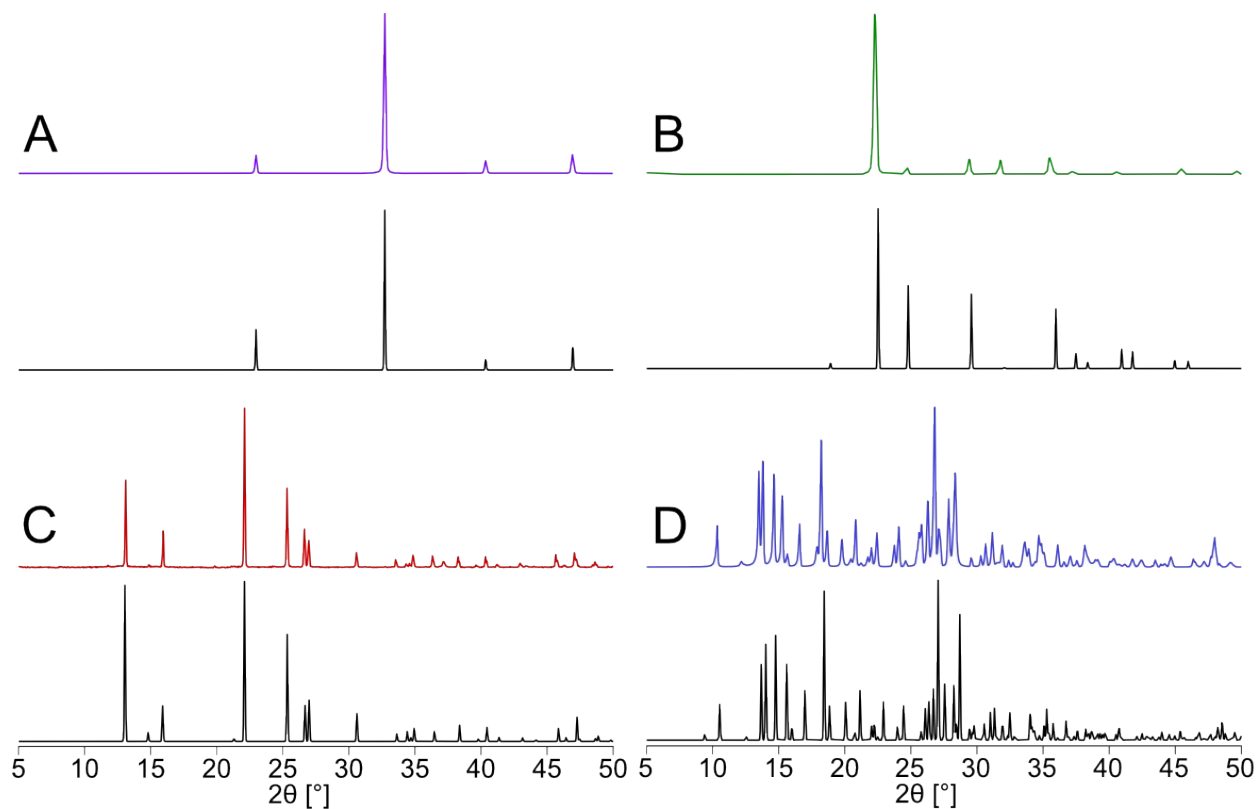


**Figure S1.** Experimental PXRD patterns for (A, purple)  $\text{NH}_4\text{Cl}$ , (B, green) urea, (C, red)  $\text{NPr}_4\text{Cl}$ , and (D, blue)  $\text{NEt}_4\text{Cl}\cdot\text{H}_2\text{O}$ , as well as simulated PXRD patterns based on previously reported or novel crystal structures (black).<sup>109,111</sup>

**Table S1.** Experimental conditions used in ball milling experiments<sup>a</sup> for the syntheses of all MCCs described in this work. All reactions were scaled to *ca.* 200 mg of total solids.

Material	NR <sub>4</sub> Cl <sup>b</sup> (mol. eq.)	Urea (mol. eq.)	Water (mol. eq.)	Water ( $\mu$ L)	Frequency (Hz)	Optimized Milling Time (min)
NEt <sub>4</sub> Cl:2Urea	1	2	0	0	30	1
NEt <sub>4</sub> Cl:Urea·2H <sub>2</sub> O	1	1	0	0	30	40
NEt <sub>4</sub> Cl:Urea·2H <sub>2</sub> O	1	1	1	18	30	40
NEt <sub>4</sub> Cl:Urea·2H <sub>2</sub> O	1	1	2	36	30	40
NPr <sub>4</sub> Cl:2Urea	1	2	0	0	30	1
NPr <sub>4</sub> Cl:3Urea	1	3	0	0	30	1
NH <sub>4</sub> Cl:Urea	1	1	0	0	30	10

<sup>a</sup> All five MCCs were prepared mechanochemically with a constant milling frequency of 30 Hz and various milling durations. After each milling duration, a sample of the product was collected for PXRD and comparison to simulations of the educts and final products to determine the optimal milling time for each reaction.

<sup>b</sup> R = H, Et, or *n*-Pr.

**Supplement S1. Euler Angle Conventions.** There are numerous discrepant Euler angle conventions for describing the relative orientation of chemical shift and EFG tensors that are used in various software packages for simulating solid-state NMR spectra, as well as for comparing relative orientations of these tensors obtained from quantum chemical computations. This is further exacerbated by inconsistencies in how the relative magnitudes of the principal components of these tensors are defined, as well as variation in related conventions for describing anisotropy and reduced anisotropy for the CS tensor, and the asymmetry parameter of the EFG tensor.

For the purposes of the current work, we have utilized ssNake 1.3 to obtain precision fits of our experimental data, where the Euler angles follow the ZX'Z'' convention. In order to make direct comparisons with relative CS and EFG tensor orientations extracted from CASTEP output files using EFGShield software, which uses the ZY'Z'' convention, we have converted the Euler angles from ssNake to the ZY'Z'' convention, according to:

$$\begin{aligned}\alpha(\text{ssNake}) &= \gamma(\text{WSOLIDS}) + 90^\circ \\ \beta(\text{ssNake}) &= \beta(\text{WSOLIDS}) \\ \gamma(\text{ssNake}) &= \alpha(\text{WSOLIDS})\end{aligned}$$

Furthermore, we verified the equivalence of these sets of Euler angles with a second set of simulations using WSOLIDS software, which is well-documented in terms of its use of the ZY'Z'' convention and the aforementioned CS and EFG tensor parameters.

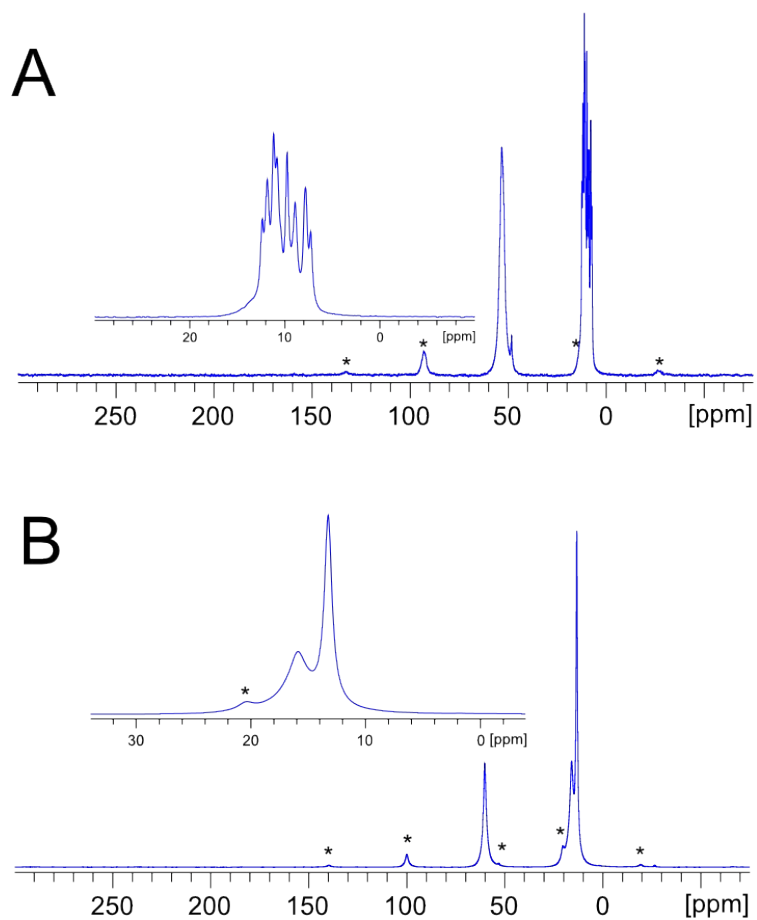


**Figure S2.** Experimental  $^1\text{H} \rightarrow ^{13}\text{C}\{^1\text{H}\}$  CP/MAS spectra for (A)  $\text{NEt}_4\text{Cl} \cdot \text{H}_2\text{O}$  and (B)  $\text{NPr}_4\text{Cl}$  acquired at 14.1 T ( $\nu_{\text{rot}} = 6$  kHz). Spinning sidebands are denoted by asterisks (\*).

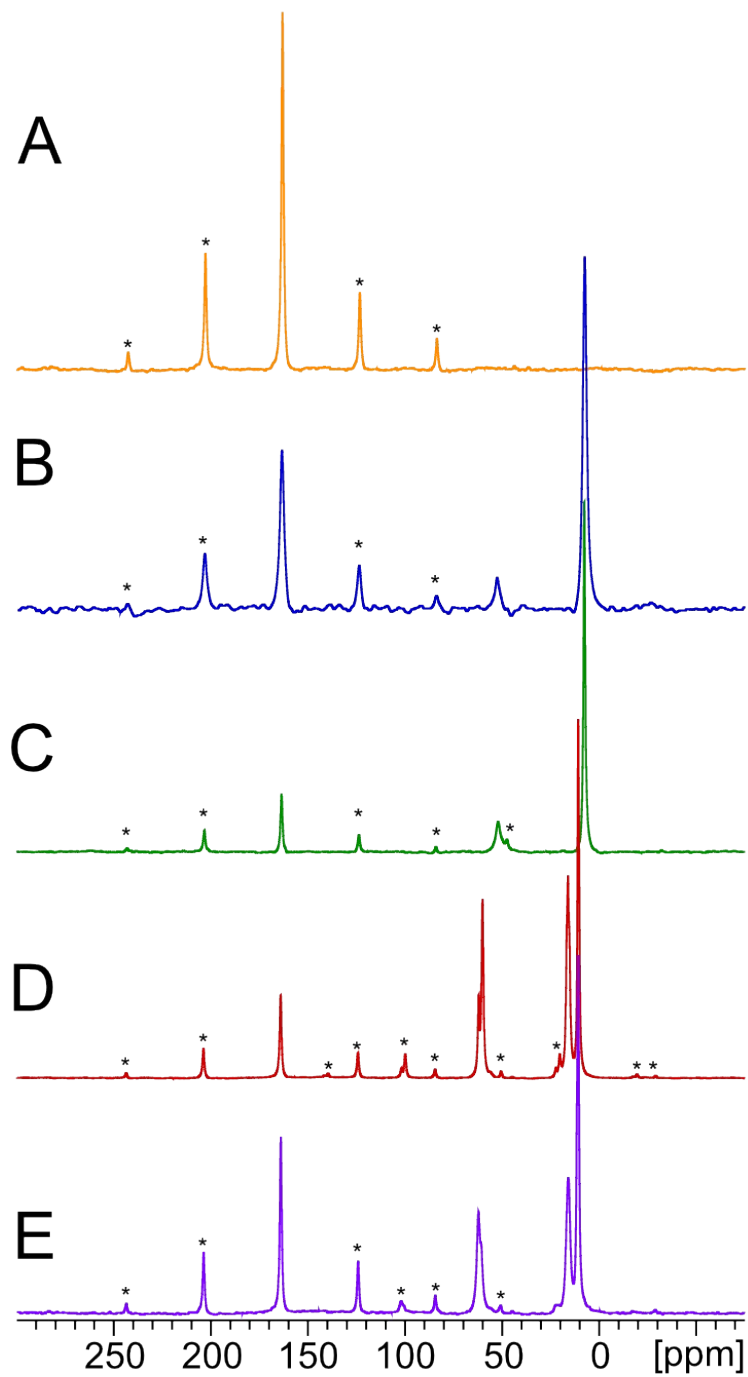


**Figure S3.** Experimental  $^1\text{H} \rightarrow ^{13}\text{C}\{^1\text{H}\}$  CP/MAS spectra of (A)  $\text{NH}_4\text{Cl}:\text{Urea}$ , (B)  $\text{NEt}_4\text{Cl}:\text{2Urea}$ , (C)  $\text{NEt}_4\text{Cl}:\text{Urea} \cdot 2\text{H}_2\text{O}$ , (D)  $\text{NPr}_4\text{Cl}:\text{2Urea}$ , and (E)  $\text{NPr}_4\text{Cl}:\text{3Urea}$  acquired at 14.1 T ( $\nu_{\text{rot}} = 6$  kHz). Spinning sidebands are denoted by asterisks (\*).

**Table S2.** Summary of experimental  $^{13}\text{C}$  chemical shifts.

Sample	Urea (ppm)	$\text{CH}_2$ (ppm)	$\text{CH}_3$ (ppm)
Urea	162.7	-	-
$\text{NEt}_4\text{Cl}\cdot\text{H}_2\text{O}$	n/a	48.2, 53.2	7.3, 7.8, 8.9, 9.7, 10.8, 11.2, 11.8, 12.4
$\text{NPr}_4\text{Cl}$	n/a	15.9, 60.2	13.3
$\text{NH}_4\text{Cl}:\text{Urea}$	163.3	n/a	n/a
$\text{NEt}_4\text{Cl}:2\text{Urea}$	163.8	52.3	7.8
$\text{NEt}_4\text{Cl}:\text{Urea}\cdot 2\text{H}_2\text{O}$	163.7	53.0	7.9
$\text{NPr}_4\text{Cl}:2\text{Urea}$	164.1	60.1, 62.1	10.9, 16.1
$\text{NPr}_4\text{Cl}:3\text{Urea}$	163.9	60.7, 62.1	10.8, 15.9

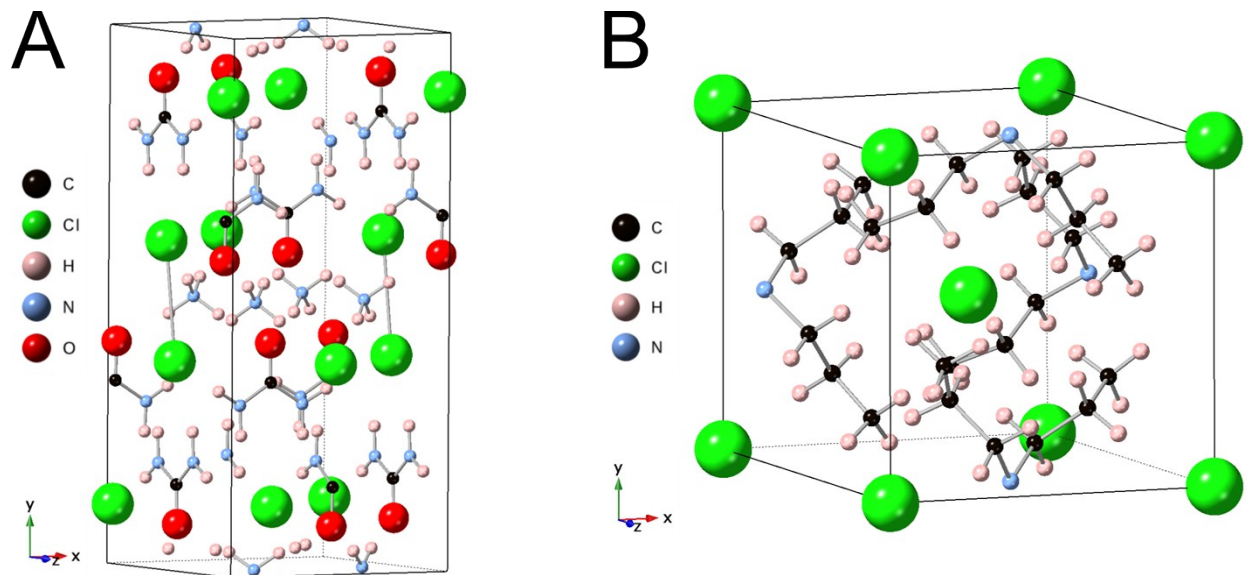


**Figure S4.** Images of the unit cells of (A)  $\text{NH}_4\text{Cl}:\text{Urea}$  and (B)  $\text{NPr}_4\text{Cl}$ .

**Table S3.** Crystal structure details for NH<sub>4</sub>Cl:Urea and NPr<sub>4</sub>Cl.

Material	NH <sub>4</sub> Cl:Urea	NPr <sub>4</sub> Cl
Empirical formula	CH <sub>8</sub> ClN <sub>3</sub> O	C <sub>12</sub> H <sub>28</sub> ClN
Formula weight (Da)	113.55	221.81
Crystal system	Orthorhombic	Tetragonal
Space group	<i>Pmna</i>	74
<i>a</i> (Å)	7.8835(4)	8.0736(8)
<i>b</i> (Å)	17.0669(8)	8.0736(8)
<i>c</i> (Å)	8.0099(3)	10.6690(10)
$\alpha, \beta, \gamma$ (°)	90	90
Cell volume (Å <sup>3</sup> )	1077.71(8)	695.44(16)
Calculated density (g cm <sup>-3</sup> )	1.3996	1.0593
Temperature (K)	170(2)	150(2)
Cell formula units, <i>Z</i>	8	1
Cell asymmetric unit, <i>Z'</i>	1	0.25
No. of unique reflections	1294	802
Final R <sub>1</sub> values ( $I > 2\sigma(I)$ )	0.0312	0.0225
Final $wR(F^2)$ values (all data) <sup>a</sup>	0.0815	0.0573

<sup>a</sup>  $wR(F^2)$  is the weighted *R* factor ( $wR$ ) based on the intensities ( $F^2$ )

**Table S4.** Experimental  $^{35}\text{Cl}$  EFG and CS tensor parameters for  $\text{NEt}_4\text{Cl}\cdot\text{H}_2\text{O}$ .<sup>a</sup>

Material (Cl Site)	Site #	$C_Q$ (MHz)	$\eta_Q$	$\delta_{\text{iso}}$ (ppm)	$\Omega$ (ppm)	$\kappa$	$\alpha$ ( $^\circ$ )	$\beta$ ( $^\circ$ )	$\gamma$ ( $^\circ$ )
$\text{NEt}_4\text{Cl}\cdot\text{H}_2\text{O}$	1	1.35(7)	0.71(6)	51(1)	24(6)	0.87(10)	n/a <sup>b</sup>	28(5)	77(15)
	2	2.51(4)	0.68(5)	68(1)	8(6)	0.44(10)	n/a	0(15)	69(24)
	3	1.18(5)	0.77(4)	60(1)	25(5)	0.10(6)	63(20)	31(20)	63(18)

<sup>a</sup> A minimum of three overlapping patterns is required to fit these spectra, although  $^{13}\text{C}$  CPMAS spectra suggest that as many as eight magnetically distinct chlorine sites could be present (see **Figure S2**).

<sup>b</sup> This parameter has little-to-no effect on the simulated  $^{35}\text{Cl}$  SSNMR pattern.

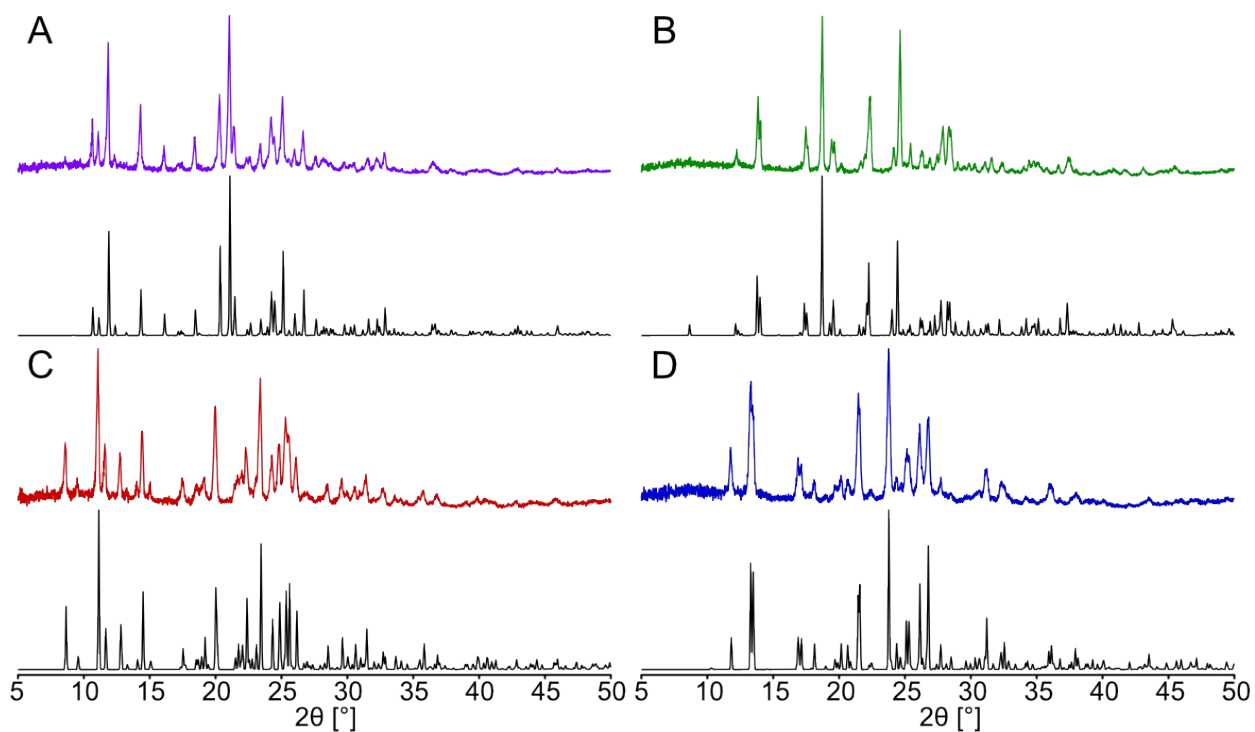


**Figure S5.** Experimental PXRD patterns for (A, purple)  $\text{NPr}_4\text{Cl}:3\text{Urea}$ , (B, green)  $\text{NEt}_4\text{Cl}:\text{Urea}\cdot 2\text{H}_2\text{O}$ , (C, red)  $\text{NPr}_4\text{Cl}:2\text{Urea}$ , and (D, blue)  $\text{NEt}_4\text{Cl}:2\text{Urea}$ , as well as simulated PXRD patterns based on previously-reported crystal structures (black).<sup>112-114</sup>

**Table S5.** Summary of crystallographic details for all  $\text{NR}_4\text{Cl} \cdot x\text{Urea} \cdot y\text{H}_2\text{O}$  MCCs and precursors discussed in this work.

Material	CSD Code	Space Group	<i>a</i> (Å)	<i>b</i> (Å)	<i>c</i> (Å)
$\text{NH}_4\text{Cl}$	n/a	$Pm\bar{3}m$	3.868	3.868	3.868
$\text{NPr}_4\text{Cl}$	This work	$I\bar{4}$	8.0736(8)	8.0736(8)	10.669(1)
$\text{NEt}_4\text{Cl} \cdot \text{H}_2\text{O}$	ETAMCM01	$C2/c$	13.4626(3)	14.1128(3)	12.1080(2)
$\text{NEt}_4\text{Cl} \cdot 2\text{Urea}$	PAMLAQ	$P2_1/c$	10.492(6)	14.954(8)	10.335(6)
$\text{NEt}_4\text{Cl} \cdot \text{Urea} \cdot 2\text{H}_2\text{O}$	GILBAE	$P2_1/n$	7.505(2)	14.556(4)	14.453(3)
$\text{NPr}_4\text{Cl} \cdot 2\text{Urea}$	NISPAG	$P2_1/n$	9.839(2)	15.160(3)	14.583(3)
$\text{NPr}_4\text{Cl} \cdot 3\text{Urea}$	NISPEK	$P2_1/c$	9.866(2)	16.274(3)	15.277(3)
$\text{NH}_4\text{Cl} \cdot \text{Urea}$	URAMCL	$Pcnm$	8.03	17.08	7.81
$\text{NH}_4\text{Cl} \cdot \text{Urea}$	URAMCL01	$Pmna$	7.9232(10)	17.1207(17)	8.0716(11)
$\text{NH}_4\text{Cl} \cdot \text{Urea}$	URAMCL02	$Pmna$	7.909(3)	17.113(6)	8.049(3)
$\text{NH}_4\text{Cl} \cdot \text{Urea}$	This work	$Pmna$	7.8835(4)	17.0669(8)	8.0099(3)

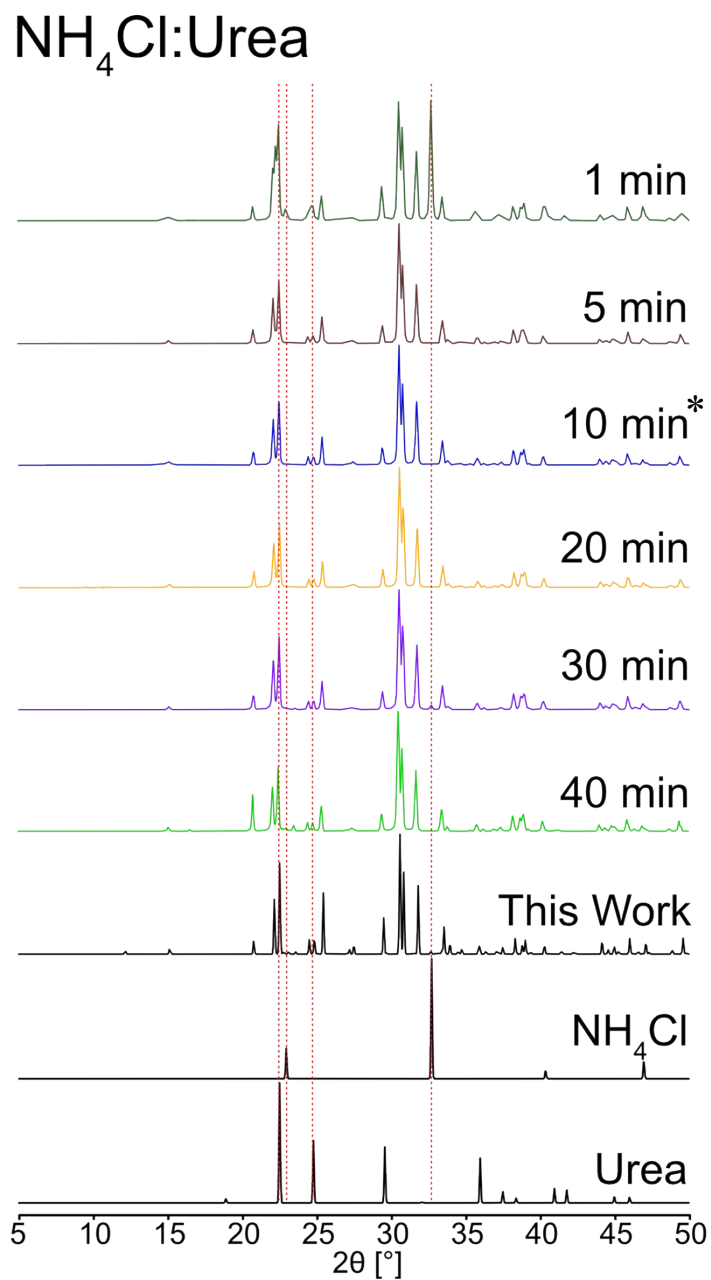


**Figure S6.** Experimental PXRD patterns for NH<sub>4</sub>Cl:Urea at 1, 5, 10, 20, 30, and 40 minutes with a constant milling frequency of 30 Hz. Optimal milling time is marked with an asterisk (\*). Simulated reference PXRD patterns for urea, NH<sub>4</sub>Cl, and NH<sub>4</sub>Cl:Urea are also shown.

# NEt<sub>4</sub>Cl:2Urea

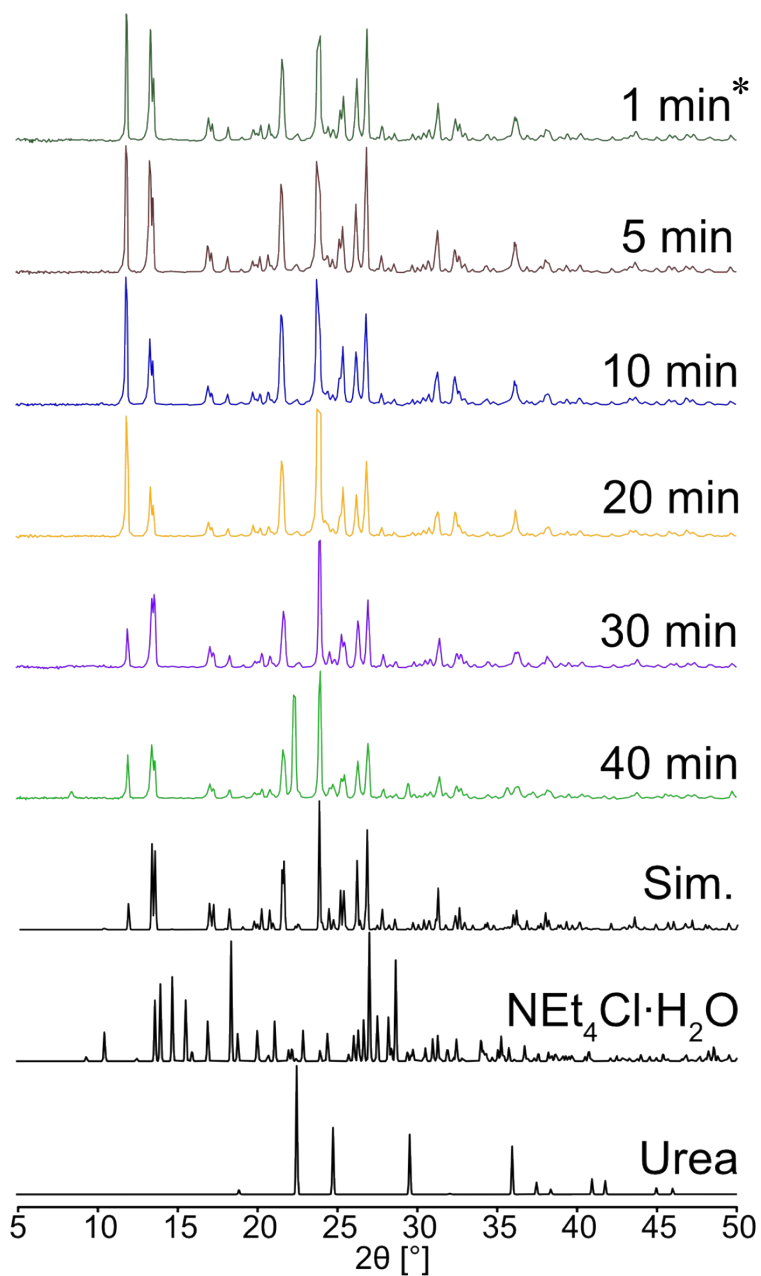


**Figure S7.** Experimental PXRD patterns for NEt<sub>4</sub>Cl:2Urea at 1, 5, 10, 20, 30, and 40 minutes with a constant milling frequency of 30 Hz. Optimal milling time is marked with an asterisk (\*). Simulated reference PXRD patterns for urea, NEt<sub>4</sub>Cl·H<sub>2</sub>O, and NEt<sub>4</sub>Cl:2Urea are also shown.

# NEt<sub>4</sub>Cl:Urea·2H<sub>2</sub>O

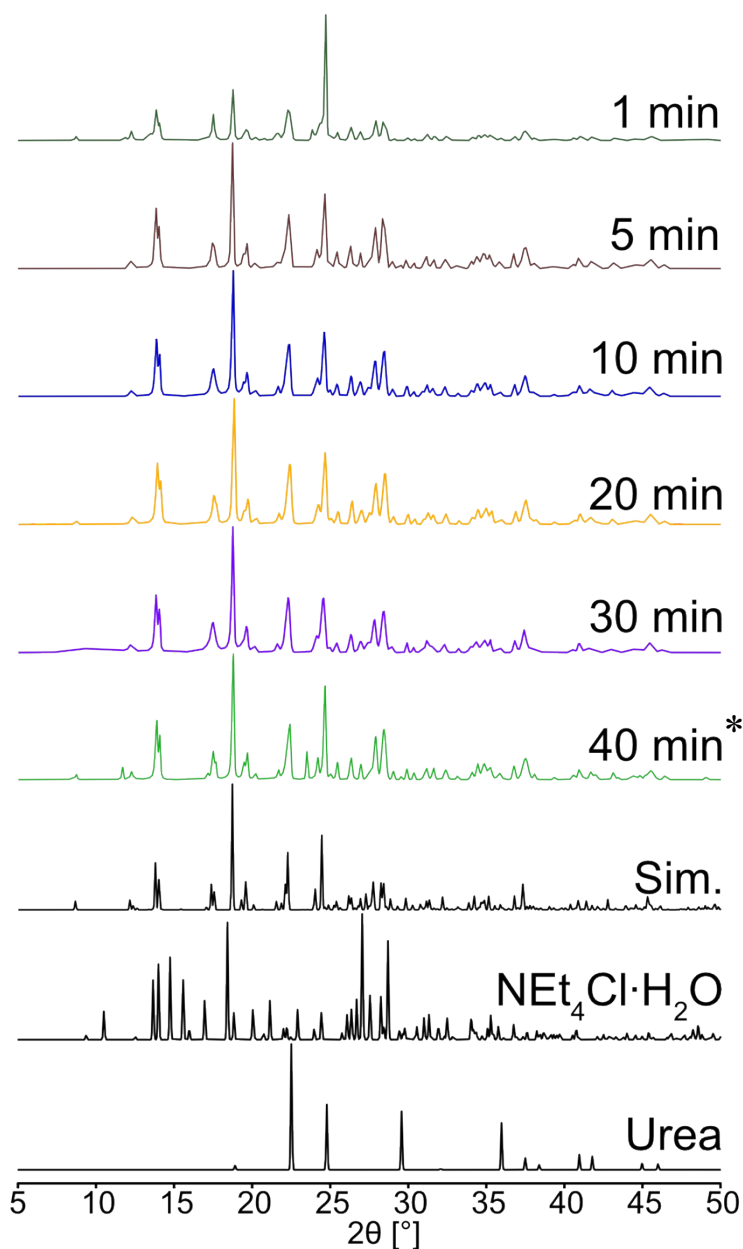


**Figure S8.** Experimental PXRD patterns for NEt<sub>4</sub>Cl:Urea·2H<sub>2</sub>O at 1, 5, 10, 20, 30, and 40 minutes with a constant milling frequency of 30 Hz. Optimal milling time is marked with an asterisk (\*). Simulated reference PXRD patterns for urea, NEt<sub>4</sub>Cl·H<sub>2</sub>O, and NEt<sub>4</sub>Cl:Urea·2H<sub>2</sub>O are also shown.

# $\text{NPr}_4\text{Cl}:2\text{Urea}$

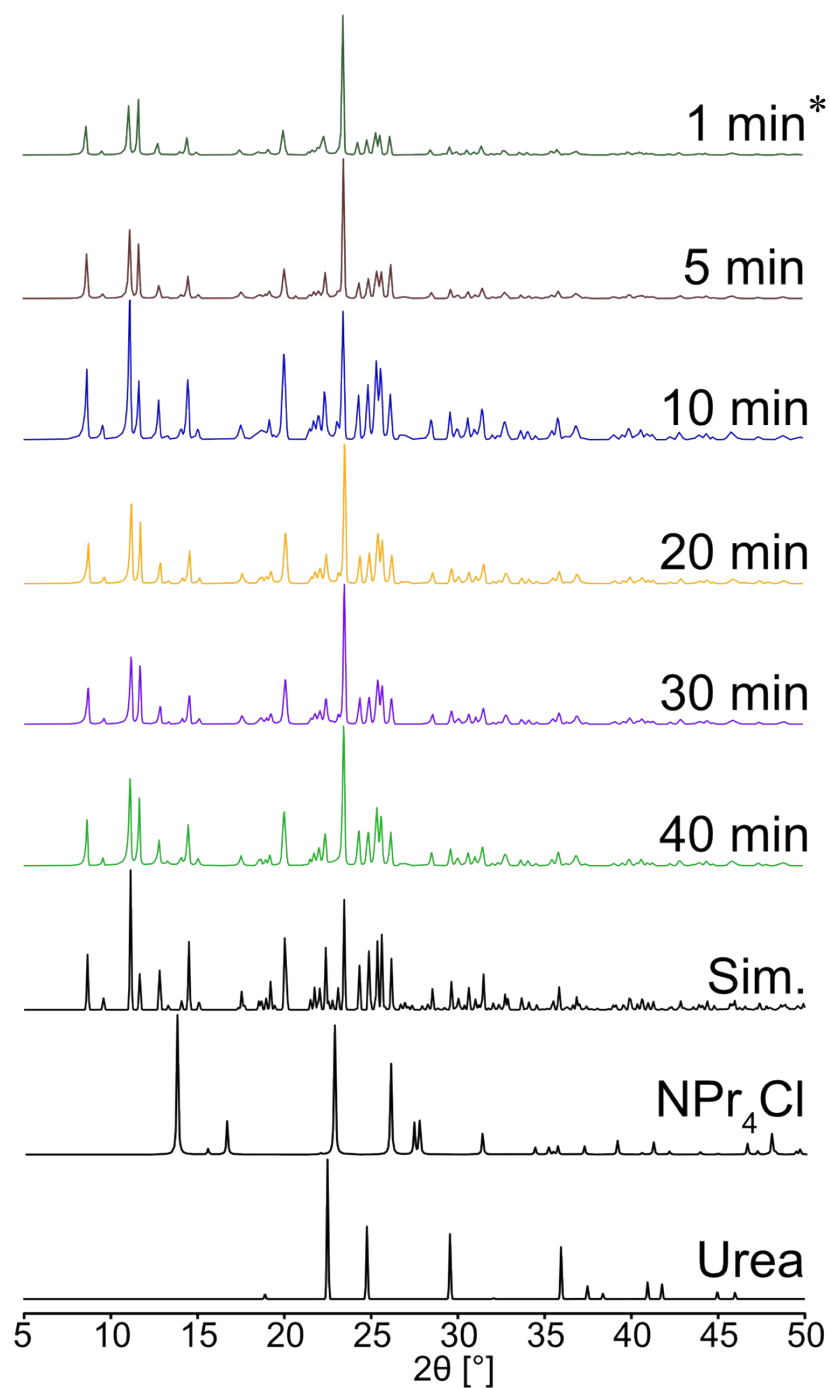


**Figure S9.** Experimental PXR D patterns for  $\text{NPr}_4\text{Cl}:2\text{Urea}$  at 1, 5, 10, 20, 30, and 40 minutes with a constant milling frequency of 30 Hz. Optimal milling time is marked with an asterisk (\*). Simulated reference PXR D patterns for urea,  $\text{NPr}_4\text{Cl}$ , and  $\text{NPr}_4\text{Cl}:2\text{Urea}$  are also shown.

# $\text{NPr}_4\text{Cl}:3\text{Urea}$

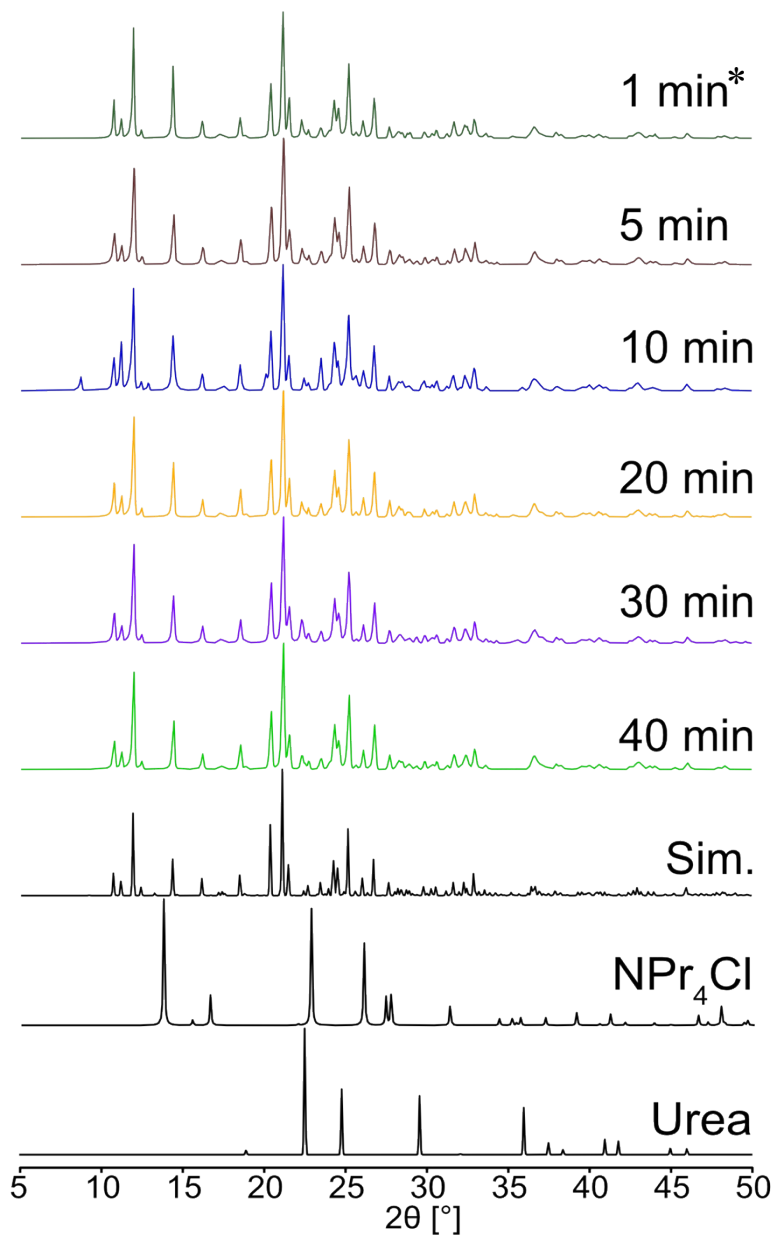


**Figure S10.** Experimental PXR D patterns for  $\text{NPr}_4\text{Cl}:3\text{Urea}$  at 1, 5, 10, 20, 30, and 40 minutes with a constant milling frequency of 30 Hz. Optimal milling time is marked with an asterisk (\*). Simulated reference PXR D patterns for urea,  $\text{NPr}_4\text{Cl}$ , and  $\text{NPr}_4\text{Cl}:3\text{Urea}$  are also shown.

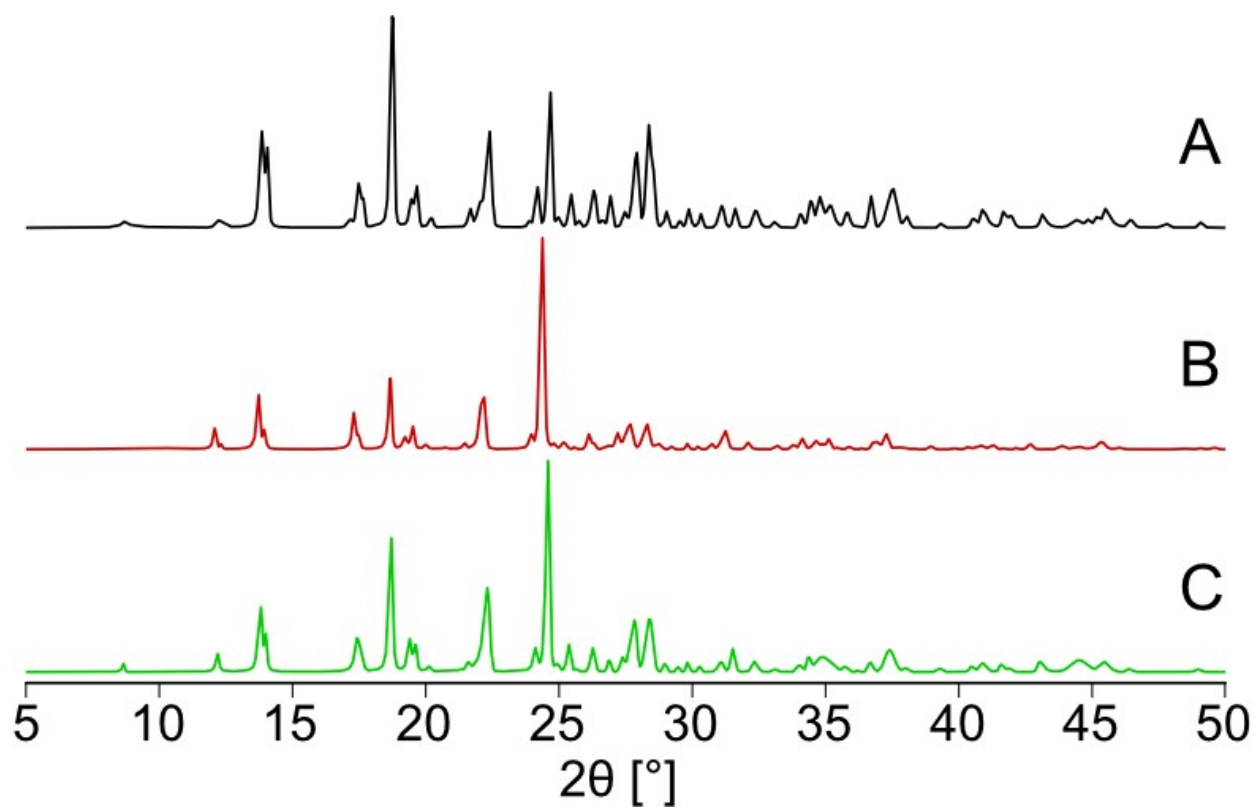


**Figure S11.** PXRD patterns of the mechanochemically synthesized product of 1 molar eq. urea, 1 molar eq.  $\text{NEt}_4\text{Cl}\cdot\text{H}_2\text{O}$ , and 0 (A), 1 (B), and 2 (C) molar eq.  $\text{H}_2\text{O}$ .

**Supplement S2. Definition of the RMS EFG Distance.** The EFG distance and RMS EFG distance are metrics introduced by our laboratory [*J. Phys. Chem. A* **2020**, *124*, 10312-10323.] for assessing the agreement between experimental and calculated EFG tensors, and is used in a similar manner to the chemical shift distance and RMS chemical shift difference introduced by Alderman et al. [*J. Magn. Reson.* **1993**, *101*, 188-197]. We assess the agreement between an experimental ( $V_{kk}^{m,exp}$ ,  $k = 1, 2, 3$ ) and calculated ( $V_{kk}^{m,calc}$ ) EFG tensor at nucleus  $m$  using the EFG distance ( $\Gamma_m$ ) metric. The EFG distance quantifies the degree of similarity between two sets of the principal components of EFG tensors (here, one experimental and one computed set of tensors) using a single scalar value (in a.u.):

$$\Gamma_m = \frac{eQ}{h} \left( \frac{1}{15} [3\Delta_{11}^2 + 3\Delta_{22}^2 + 3\Delta_{33}^2 + 2\Delta_{11}\Delta_{22} + 2\Delta_{11}\Delta_{33} + 2\Delta_{22}\Delta_{33}] \right)^{1/2}.$$

$$\Delta_{kk} = \left| \left| V_{kk}^{m,calc} \right| - \left| V_{kk}^{m,exp} \right| \right|.$$

In the above expressions,  $e$  is the elementary charge,  $h$  is Planck's constant, and  $Q$  is the nuclear quadrupole moment [ $Q(^{14}\text{N}) = 2.044 \text{ fm}^2$ ;  $Q(^{35}\text{Cl}) = -8.165 \text{ fm}^2$ ]. A root-mean-square EFG distance for an ensemble of  $M$  EFG tensors ( $\Gamma_{RMS}$ ) is determined by the following expression:

$$\Gamma_{RMS} = \left( \frac{1}{M} \sum_m \Gamma_m^2 \right)^{1/2}.$$

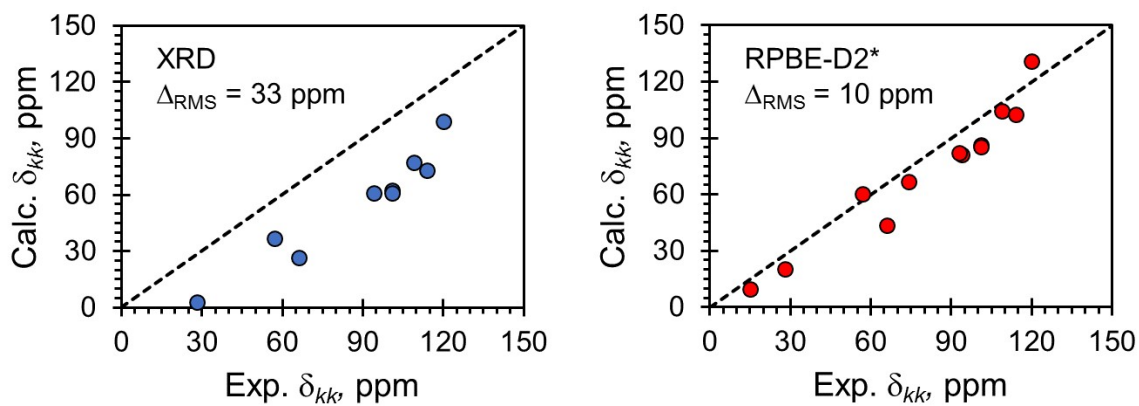


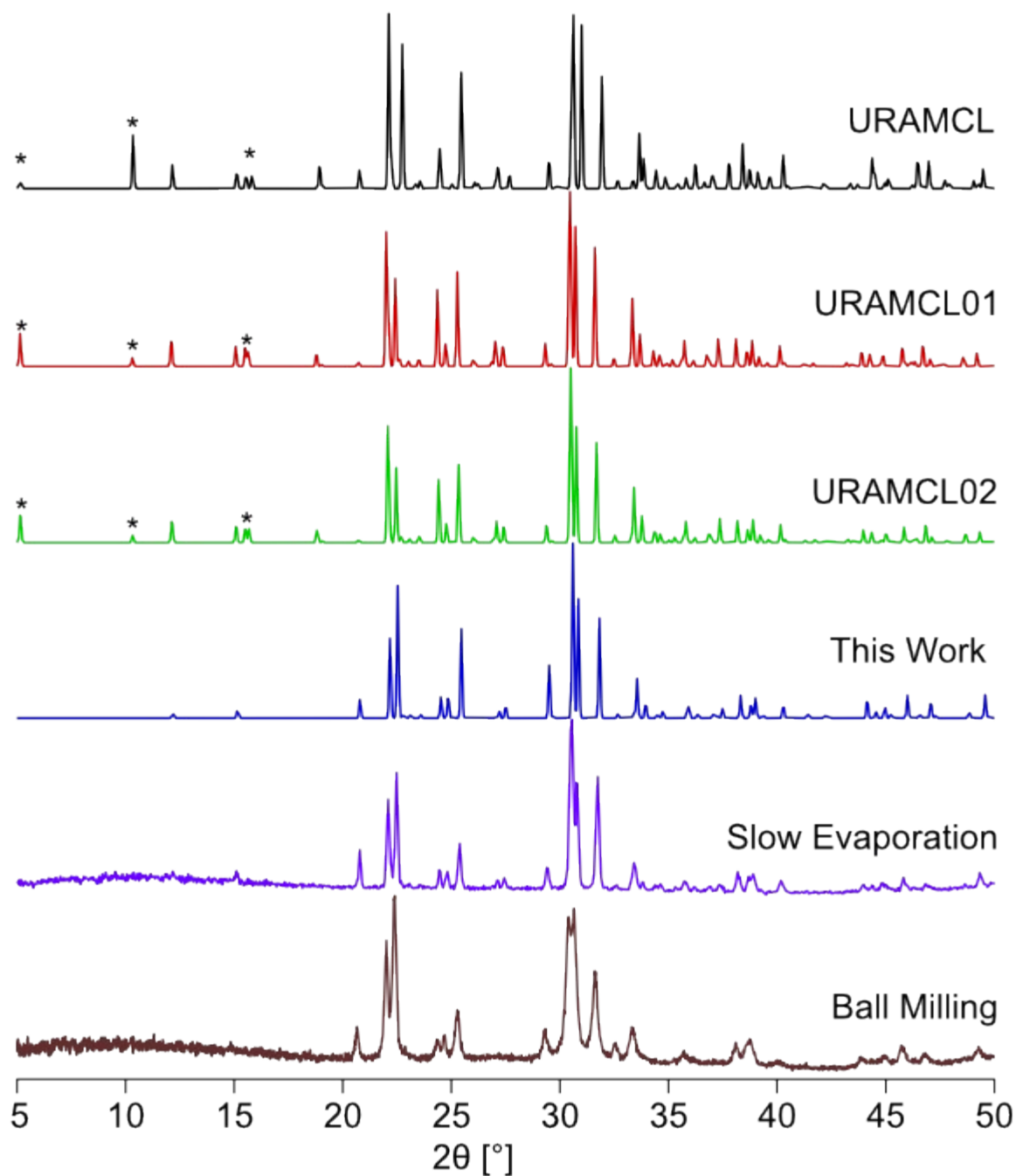
**Figure S12.** Correlations between calculated and experimental principal values of  $^{35}\text{Cl}$  chemical shift tensors for tetraethyl and tetrapropyl  $\text{NR}_4\text{Cl}:x\text{Urea}\cdot y\text{H}_2\text{O}$  MCCs. Calculations are shown for XRD-derived structures (blue) and DFT-D2\* structures (red).

**Supplement S3. Definition of the RMS CS Distance.** The chemical shift distance [J. Magn. Reson. 1993, 101, 188-197] for atom  $v$ ,  $d_v$ , is used to compare a calculated and experimental chemical shift tensors:

$$d_v = \left( \frac{1}{15} \left[ 3(\delta_{11}^{v,calc} - \delta_{11}^{v,exp})^2 + 3(\delta_{22}^{v,calc} - \delta_{22}^{v,exp})^2 + 3(\delta_{33}^{v,calc} - \delta_{33}^{v,exp})^2 + 2(\delta_{11}^{v,calc} - \delta_{11}^{v,exp})(\delta_{22}^{v,calc} - \delta_{22}^{v,exp}) + 2(\delta_{11}^{v,calc} - \delta_{11}^{v,exp})(\delta_{33}^{v,calc} - \delta_{33}^{v,exp}) + 2(\delta_{22}^{v,calc} - \delta_{22}^{v,exp})(\delta_{33}^{v,calc} - \delta_{33}^{v,exp}) \right] \right)^{1/2}$$

A root-mean-square (RMS) chemical shift distance for an ensemble of  $N$  chemical shift tensors ( $\Delta_{RMS}$ ) is determined by the following expression:

$$\Delta_{RMS} = \left( \frac{1}{N} \sum_{v=1}^N d_v^2 \right)^{1/2}$$



\* Indicates unique reflections that are not present in the experimental PXRD.

**Figure S13.** Experimental and simulated PXRD patterns of products from MS and crystallization from solution, as well as simulated PXRD patterns for  $\text{NH}_4\text{Cl}:\text{Urea}$ . Both slow evaporation (purple) and ball milling (brown) products from preparations of  $\text{NH}_4\text{Cl}:\text{Urea}$  are compared to simulations of the three reported crystal structures, black (URAMCL), red (URAMCL01), and green (URAMCL02),<sup>123–125</sup> and our *Pmna* crystal structure (blue).

**Table S6.** Calculated  $^{35}\text{Cl}$  EFG tensor parameters for all available structures of  $\text{NH}_4\text{Cl}:\text{Urea}$ , as refined at the DFT-D2\* level.

CCSD Code	Space Group	Temp (K)	Energy (kJ/mol)	C11		C12	
				$C_Q$ (MHz)	$\eta_Q$	$C_Q$ (MHz)	$\eta_Q$
URAMCL <sup>a</sup>	<i>Pcnm</i>	298	-	-	-	-	-
URAMCL01	<i>Pmna</i>	298	0.0	4.63	0.32	-3.32	0.53
URAMCL02	<i>Pmna</i>	298	0.2	4.63	0.32	-3.32	0.52
This Work	<i>Pmna</i>	170	0.7	4.63	0.34	-3.32	0.53

<sup>a</sup> Self-consistent field convergence was not possible for calculations using this structure.

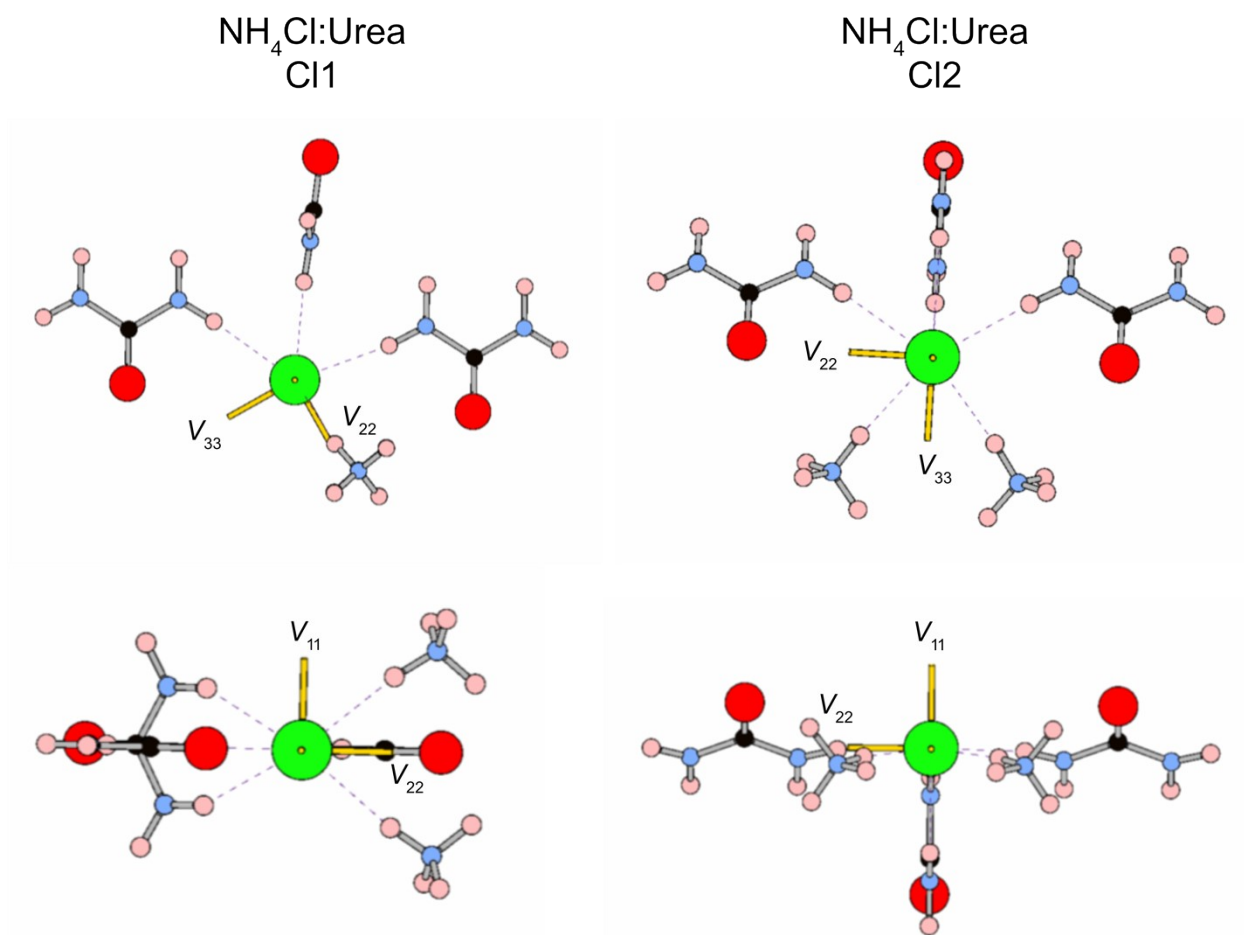


**Figure S14.** <sup>35</sup>Cl EFG tensor orientations for NH<sub>4</sub>Cl:Urea obtained from model structures from our crystal structure that were geometry optimized at the DFT-D2\* level. The H···Cl<sup>-</sup> hydrogen bonds (< 2.6 Å) are shown in black. The orientations of the three principal components of the EFG tensor ( $V_{11}$ ,  $V_{22}$ , and  $V_{33}$ ) are shown in yellow.

**Table S7.** Acquisition parameters for all  $^{35}\text{Cl}\{^1\text{H}\}$  Hahn-echo SSNMR spectra.

Material	$B_0$ (T)	$\nu_{\text{rot}}$ (kHz)	Time Domain	Spectral Width (kHz)	Dwell Time ( $\mu\text{s}$ )	Acquisition Time (ms)	Recycle Delay (s)	CT-sel. $\pi/2$ pulse width ( $\mu\text{s}$ ) <sup>a</sup>	$^1\text{H}$ decoupling (kHz)	Scans
NEt <sub>4</sub> Cl:2Urea	9.4	0	2048	125	4.00	8.192	0.5	5.0	25	12288
	9.4	12	3072	150	3.33	10.24	0.5	2.0	25	5920
	19.5	0	2048	100	5.00	10.24	0.5	8.0	55	11264
	19.5	16	2048	100	5.00	10.24	0.5	8.0	55	3072
NEt <sub>4</sub> Cl:Urea·2H <sub>2</sub> O	9.4	0	2048	250	2.00	4.096	0.5	2.5	25	12288
	19.5	16	2048	100	5.00	10.24	0.5	8.0	55	7168
	19.5	0	2048	100	5.00	10.24	0.5	8.0	55	86016
NPr <sub>4</sub> Cl:2Urea	9.4	0	2048	250	2.00	4.096	0.5	2.5	25	12288
	9.4	15	2048	200	2.50	5.12	0.5	2.0	25	12288
	19.5	0	2048	100	5.00	10.24	0.5	8.0	55	28672
	19.5	16	2048	100	5.00	10.24	0.5	8.0	55	6144
NPr <sub>4</sub> Cl:3Urea	9.4	0	1024	50	10.00	10.24	0.5	2.5	25	10240
	9.4	5	3072	59.5	8.40	25.804	0.5	2.0	25	3696
	19.5	0	2048	100	5.00	10.24	0.5	8.0	55	7168
	19.5	16	2048	100	5.00	10.24	0.5	8.0	55	512
NH <sub>4</sub> Cl:Urea	9.4	0	2048	250	2.00	4.096	1.0	2.5	25	7488
	19.5	0	5120	200	2.50	12.8	1.4	3.0	55	2048
	19.5	16	5120	200	2.50	12.8	1.4	3.0	55	1024
NH <sub>4</sub> Cl	9.4	0	4096	50	10.00	40.96	1.0	2.5	25	64
	9.4	5	8192	150	3.33	27.31	1.0	2.0	25	1024
NPr <sub>4</sub> Cl	9.4	0	2048	50	10.00	20.48	4.0	2.5	25	1184
	9.4	5	36864	500	1.00	36.86	4.0	4.0	25	4096
NEt <sub>4</sub> Cl·H <sub>2</sub> O	9.4	0	1024	150	3.33	3.41	1.0	2.5	25	7968
	9.4	5	3072	150	3.33	10.24	1.0	2.0	25	12288
	19.5	0	2048	100	5.00	10.24	1.0	8.0	55	7168
	19.5	16	2048	100	5.00	10.24	1.0	8.0	55	3072

<sup>a</sup> For half-integer quadrupolar nuclei, a selective pulse ( $(\pi/2)/(I+1/2)$ ) is used to selectively excite the central transition pattern

**Table S8.** Acquisition parameters for all  $^1\text{H} \rightarrow ^{13}\text{C}\{^1\text{H}\}$  CP/MAS SSNMR spectra.

Material	$B_0$ (T)	$\nu_{\text{rot}}$ (kHz)	Time Domain	Spectral Width (kHz)	Dwell Time ( $\mu\text{s}$ )	Acquisition Time (ms)	Recycle Delay (s)	$\pi/2$ pulse width ( $\mu\text{s}$ )	Contact Time (ms)	$^1\text{H}$ decoupling (kHz)	Scans
$\text{NEt}_4\text{Cl}:2\text{Urea}$	14.1	6	8192	100	5.00	40.96	6	5.0	2	100	1024
$\text{NEt}_4\text{Cl}:\text{Urea}\cdot 2\text{H}_2\text{O}$	14.1	6	8192	100	5.00	40.96	6	5.0	2	100	1024
$\text{NPr}_4\text{Cl}:2\text{Urea}$	14.1	6	8192	100	5.00	40.96	15	5.0	2	100	256
$\text{NPr}_4\text{Cl}:3\text{Urea}$	14.1	6	8192	100	5.00	40.96	30	5.0	2	100	128
$\text{NH}_4\text{Cl}:\text{Urea}$	14.1	6	8192	100	5.00	40.96	3	5.0	2	100	2048
$\text{NPr}_4\text{Cl}$	14.1	6	8192	100	5.00	40.96	6	5.0	2	100	512
$\text{NEt}_4\text{Cl}\cdot\text{H}_2\text{O}$	14.1	6	8192	100	5.00	40.96	3	5.0	2	100	1024